Electronic Supplementary Material (ESI) for ChemComm.

Supplementary information

Compositional dependence of structures and hydrogen evolution reaction activity of platinum-group-metal quinary RuRhPdIrPt alloy nanoparticles

Yuto Maruta[a], Kohei Kusada[a, b, c,*], Dongshuang Wu[a], Tomokazu Yamamoto[d], Takaaki Toriyama[d], Syo Matsumura[d, e], Okkyun Seo[f], Satoshi Yasuno[f], Shogo Kawaguchi[f], Osami Sakata[f], Yoshiki Kubota[g], Hiroshi Kitagawa[a,*]

[a]Division of Chemistry, Graduate School of Science, Kyoto University, Kitashirakawa-Oiwakecho, Sakyo-ku, Kyoto 606-8502, Japan

[b]The HAKUBI Centre for Advanced Research, Kyoto University, Kitashirakawa-Oiwakecho, Sakyo-ku, Kyoto 606-8502, Japan

[c]JST-PRESTO, Honcho 4-1-8, Kawaguchi, Saitama, 332-0012 Japan

[d]The Ultramicroscopy Research Centre, Kyushu University, Motooka 744, Nishi-ku, Fukuoka 819-0395, Japan

[e]Department of Applied Quantum Physics and Nuclear Engineering, Kyushu University, Motooka 744, Nishi-ku, Fukuoka 819-0395, Japan

[f]Center for Synchrotron Radiation Research, Japan Synchrotron Radiation Research Institute (JASRI) SPring-8, 1-1-1 Kouto, Sayo-cho, Sayo-gun, Hyogo 679-5198, Japan.

[g]Department of Physics, Graduate School of Science, Osaka Metropolitan University, Sakai, Osaka 599-8531, Japan

*Showing:

Kohei Kusada: kusada@kuchem.kyoto-u.ac.jp

Hiroshi Kitagawa: kitagawa@kuchem.kyoto-u.ac.jp

Synthesis of RuRhPdIrPt quinary alloy NPs and monometallic NPs

For the synthesis of platinum-group-metal quinary NPs, five metal precursors, $RuCl_3 \cdot nH_2O$, $RhCl_3 \cdot nH_2O$, K_2PdCl_4, K_2PtCl_4 and H_2IrCl_6 were dissolved in 15 mL of 0.1 M HCl (aq). This solution was mixed with carbon (VULCAN XC-72R 160 mg) and isopropanol (15 mL). Then, the mixture was sprayed into preheated triethylene glycol (TEG, 150 mL) solution at 220°C. After adding the mixture, the solution was kept at 220°C for 10 min and cooled to RT. The obtained NPs were separated from the solution by centrifugation with acetone and diethylene ether. After washing the NPs three times with acetone, water, and ethanol to remove impurities, the obtained black powders were vacuum-dried under RT. The metal-rich alloy NPs and monometallic NPs were obtained using a similar process by adding the corresponding metal precursors. The amounts of precursors are summarised in Table S1.

Synthesis of Pd NPs

First, 122.7 mg of K_2PdCl_4 was dissolved in 15 mL of 0.1 M HCl (aq). This solution was mixed with 5 mL of isopropanol and 160 mL of the TEG containing carbon. Then, the mixture was refluxed at 120°C for 1 h and cooled to RT. The washing process was the same as described above. The obtained Pd NPs were treated with hydrogen at 200°C.

Characterisation

HT7700 TEM (Hitachi, Japan) was used at 100 kV for taking bright-field TEM images. The atomic ratios were measured by XRF (ZSX Primus IV, Rigaku, Japan). HAADF-STEM images and elemental maps were obtained at 120 kV with an aberration corrector using a JEM-ARM200CF STEM instrument (JEOL, Japan). Synchrotron XRD patterns were measured at the beamline BL02B2 at SPring-8 in Japan with X-ray having 0.63021(2) Å of wavelength. XPS measurements using a Mg *Kα* anode were carried out with a Shimadzu ESCA-3400 X-ray photoelectron spectrometer (Shimadzu, Japan). XPS spectra were calibrated by the C 1s peak at 284.38 eV. VB spectra were measured by hard X-ray photoelectron spectroscopy (HAXPES) at the undulator beamline BL46XU at SPring-8 in Japan with the X-ray having an incident photon energy of 7.94 keV.

Hard X-ray photoelectron spectroscopy (HAXPES)

The total energy resolution was estimated to be 0.29 eV by measuring the Fermi cut-off of an evaporated Au thin film. The binding energy is considered the Fermi level of Au thin film.

For the VB spectra analyses, real background subtraction was performed by measuring the carbon powder VB spectra. All the VB spectra were normalised in the same region (0–12 eV). The *d*-band centre was obtained by using the following equation:

$$E_{d-band} = \frac{\int E \times DOS(E)dE}{\int DOS(E)dE}$$

where *E* is a binding energy and DOS(*E*) is the DOS of the occupied *d* states. Because of the small contribution of the *s* band to the VB spectrum of the *d*-metal, here we used the *I*(*E*) (intensity of a VB spectrum) to correspond to the DOS(*E*), and the centre position was defined as the centre of gravity of the VB spectra.

$$E_{d-band}^{obs} = \frac{\int E \times I(E)dE}{\int I(E)dE}$$

Electrochemical measurements

All electrochemical measurements were performed at RT and repeated three times to obtain reproducible data using an electrochemical workstation (CHI 760e, CH Instruments, USA). The electrolyte was prepared using 60% $HClO_4$ in Millipore water (>18.2 MΩ cm). The weight percentage of the metal on the carbon-loaded catalysts was calculated by elemental analysis and was about 20% for all samples. The electrocatalyst inks contained 0.5 mg/mL in metals and were prepared by dispersing the carbon-loaded NPs in a mixture of isopropanol and 0.05 wt% Nafion. The Ag/AgCl reference electrode (saturated KCl), a carbon rod and a rotating disk electrode (RDE, φ 5.0 mm) were used for the measurements. 10 μL of the catalyst ink was dropped onto the RDE surfaces and dried under air overnight at RT.

In the general procedure of HER, several hundred cycles of voltammogram (CVs) tests were carried out with a high scan speed (500 mV/s) in an Ar-saturated electrolyte to obtain a stable surface. The HER was conducted by linear scanning voltammogram technique with a rotation speed of 1600 rpm/s and a scan rate of 5 mV/s. All the data were compensated with the resistance of the solution as 85%.

The electrochemical active surface area was obtained by Cu underpotential deposition (UPD) measurement. The Cu UPD method that can be applied to all platinum group metals

was used to evaluate the surface area. Turnover frequency was calculated by using these results. First, 0.5 M H_2SO_4 and 5 mM $CuSO_4$ + 0.5 M H_2SO_4 solutions were prepared. Several hundred CV tests in the range of 0.05 V–0.40 V (vs Ag/AgCl) at a high speed (500 mV/s) were performed in an Ar-saturated 0.5 M H_2SO_4 solution to obtain a stable surface. Next, a fine CV was performed at 10 mV/s in the range of 0.05 V–0.40 V (vs Ag/AgCl) and used as a background for Cu UPD measurement. The electrode was kept at a certain potential for 100 s. CV was carried out with the anodic sweep direction from the specific potential to the limit potential of the background at the scan rate of 10 mV/s. The specified potential was defined as the potential making monolayer Cu on the surface of the catalyst. The EASA was calculated by Equation (1), and the number of *n* and TOF were also calculated by Equations (2) and (3), respectively:

$$EASA = \frac{Q_{Cu}}{0.42} = \frac{\int_{E_1}^{E_2} I(E)d(E)}{v \times 0.42} \#(1)$$

$$n = \frac{Q_{cu}}{2F} \#(2)$$

$$TOF = \frac{I}{2Fn} \#(3)$$

where Q_{Cu} is the voltammetry charge of Cu UPD calculated by the subtraction of the black CV profile in pure 0.5 M H_2SO_4. E_1 and E_2 are the lower and upper limits of the Cu UPD profile, and v is the scan speed of the CV profile (Fig. S7). 0.42 mC cm^{-2} was used as the conversion factor for the two-electron Cu deposition process. F is the Faraday constant (96480 C mol^{-1}).

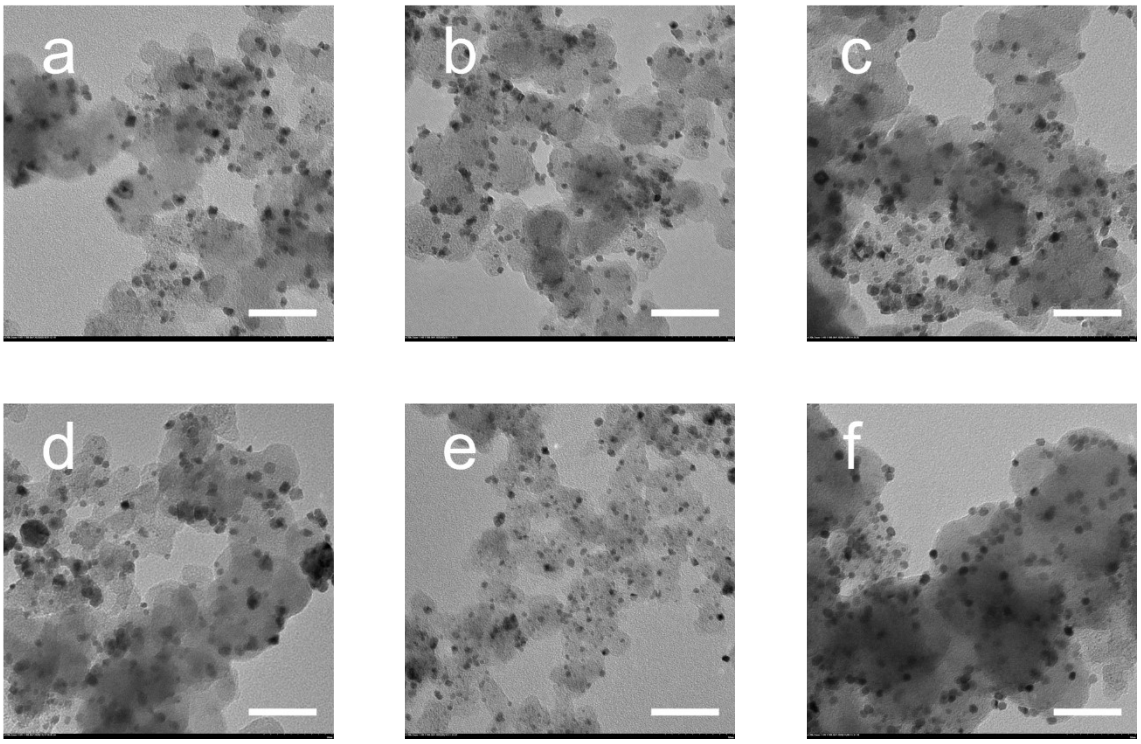

Fig. S1. Bright-field TEM images of (a) Equi, (b) Ru-rich, (c) Rh-rich, (d) Pd-rich, (e) Ir-rich and (f) Pt-rich alloy NPs. The scale bars show 50 nm in all the samples. The average particle sizes of the obtained alloy NPs were 4.6 ± 1.7, 3.6 ± 1.6, 4.0 ± 1.6, 4.6 ± 2.0, 3.0 ± 0.7 and 4.4 ± 1.7 nm, respectively.

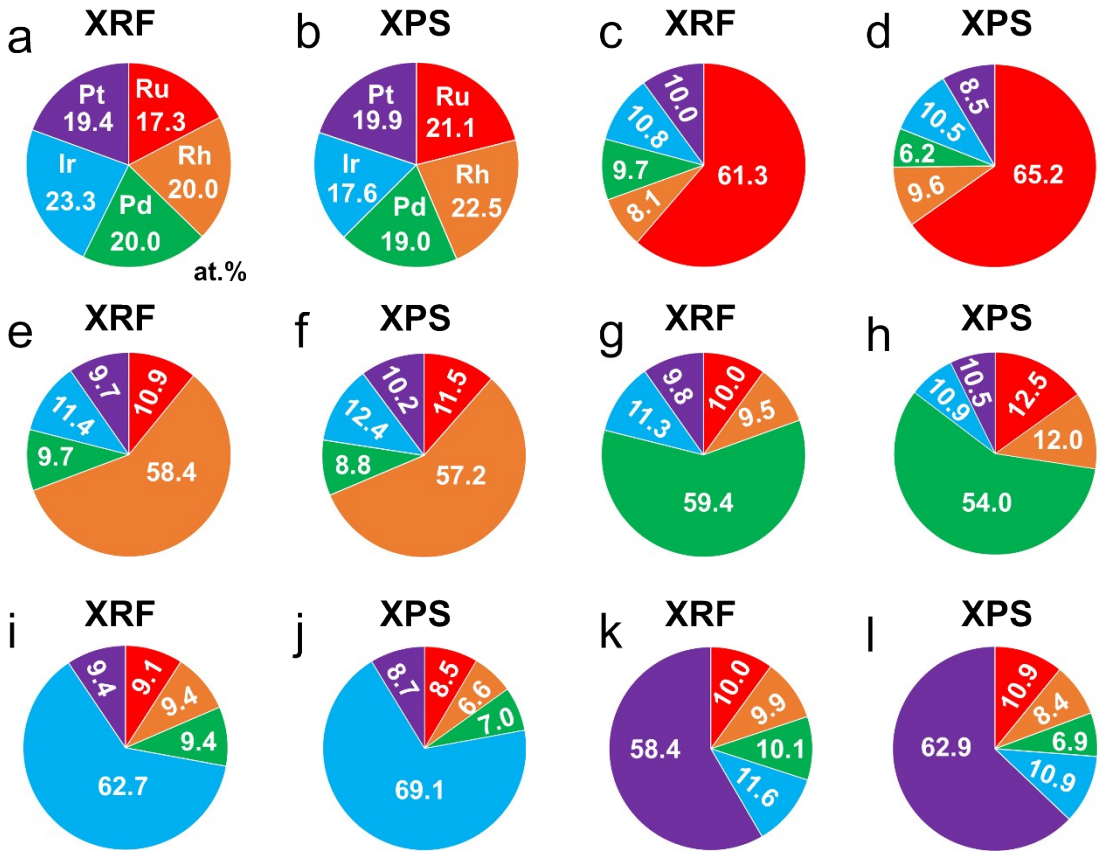

Fig. S2. Composition of (a and b) Equi, (c and d) Ru-rich, (e and f) Rh-rich, (g and h) Pd-rich, (i and j) Ir-rich and (k and l) Pt-rich alloy NPs calculated from XRF and XPS.

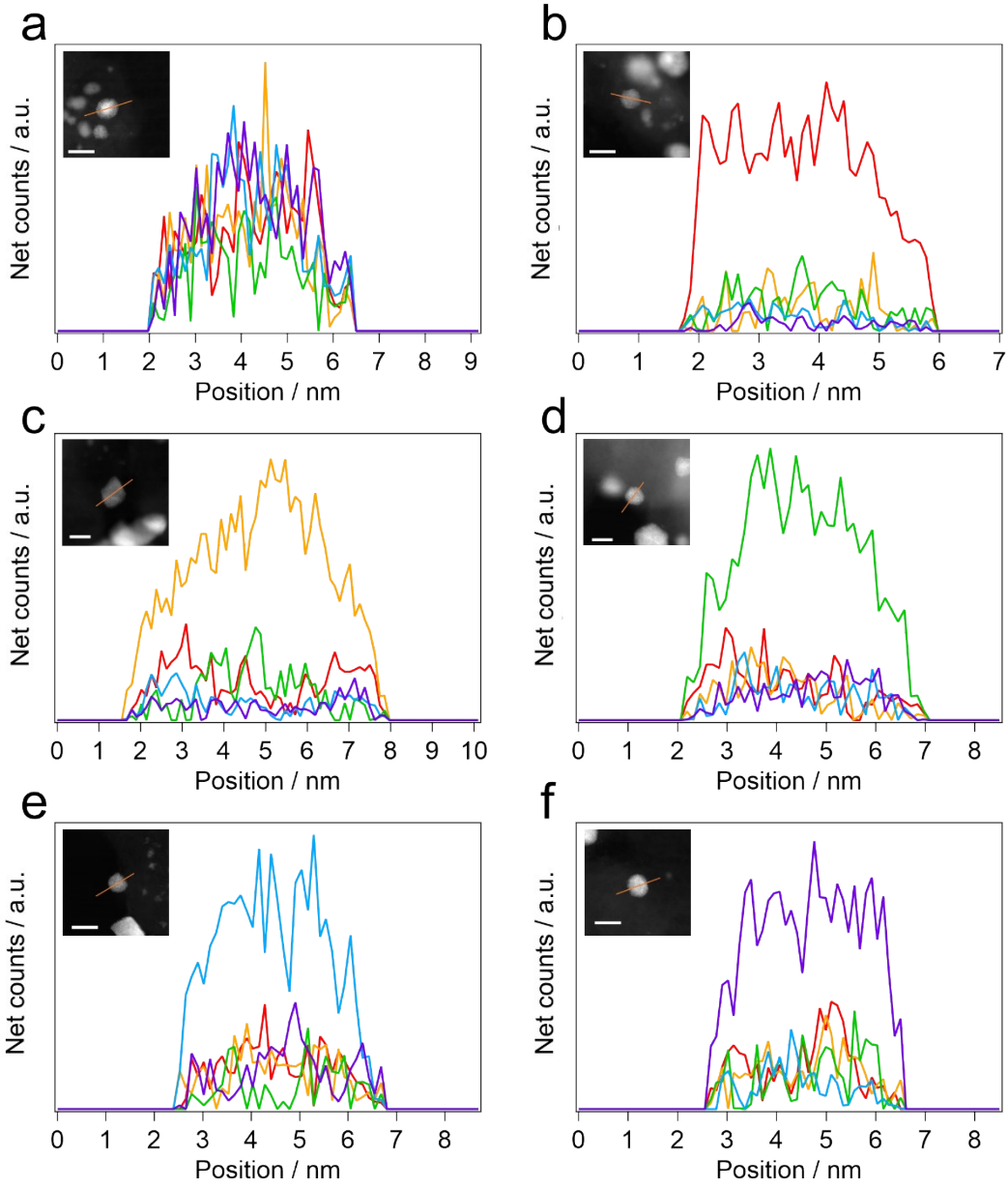

Fig. S3. STEM EDX line profiles and corresponding NPs of (a) Equi, (b) Ru-rich, (c) Rh-rich, (d) Pd-rich, (e) Ir-rich, (f) Pt-rich alloy NPs. The scale bars show 5 nm in all the samples.

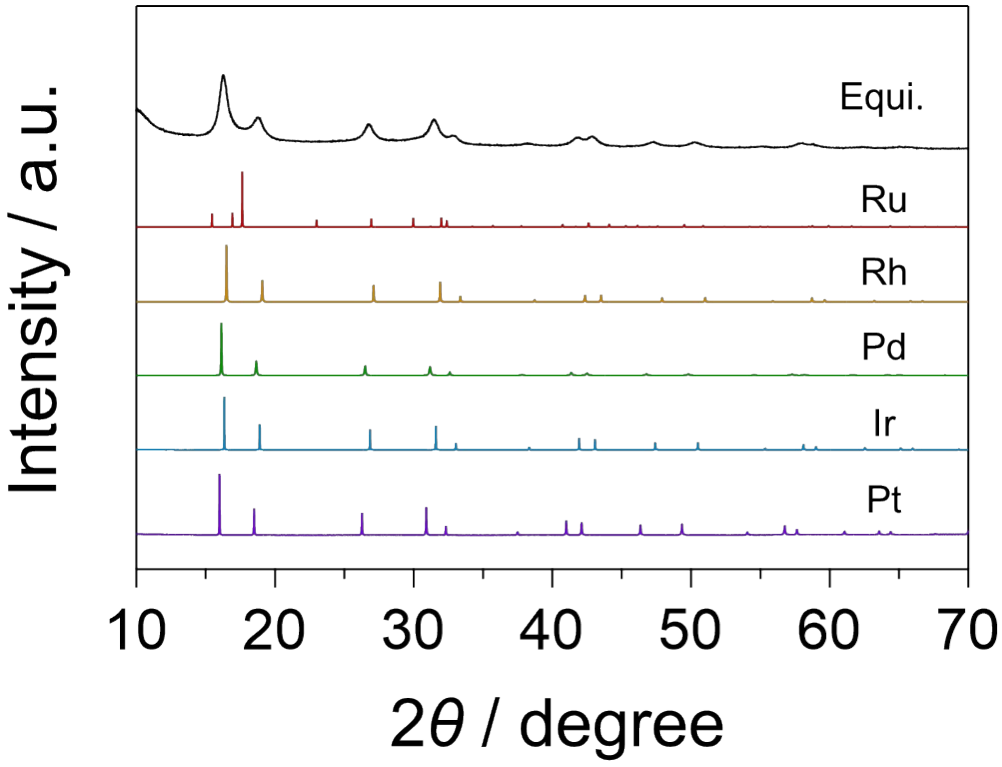

Fig. S4. PXRD patterns of Equimolar alloy NPs, Ru, Rh, Pd, Ir, Pt bulks.

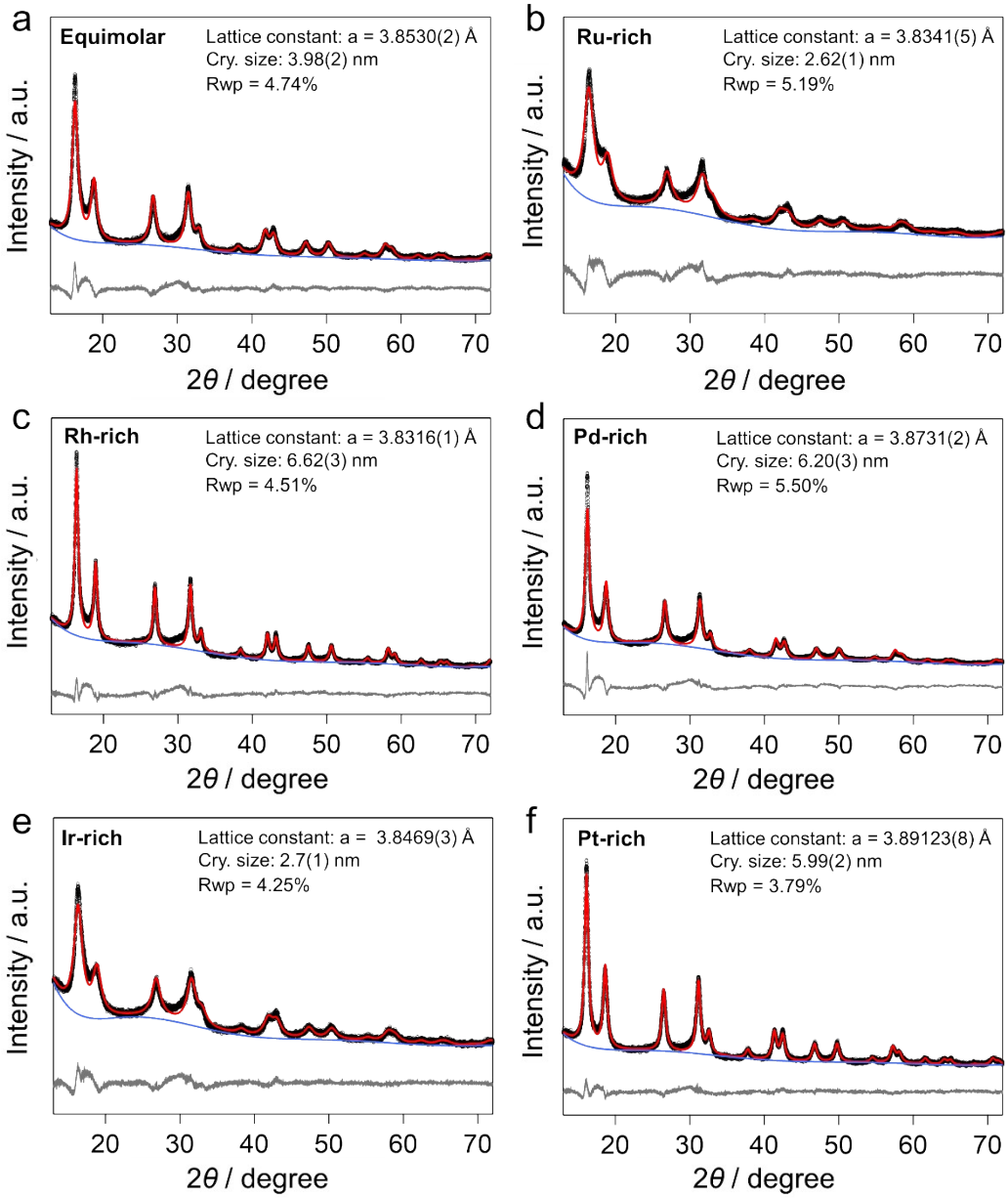

Fig. S5. Rietveld refinement of synchrotron XRD patterns of (a) Equi, (b) Ru-rich, (c) Rh-rich, (d) Pd-rich, (e) Ir-rich and (f) Pt-rich alloy NPs. The raw data, fitting profiles, background and residual curves are shown as black circles, and red, blue and grey curves, respectively. Wavelength: λ = 0.63021(2) Å.

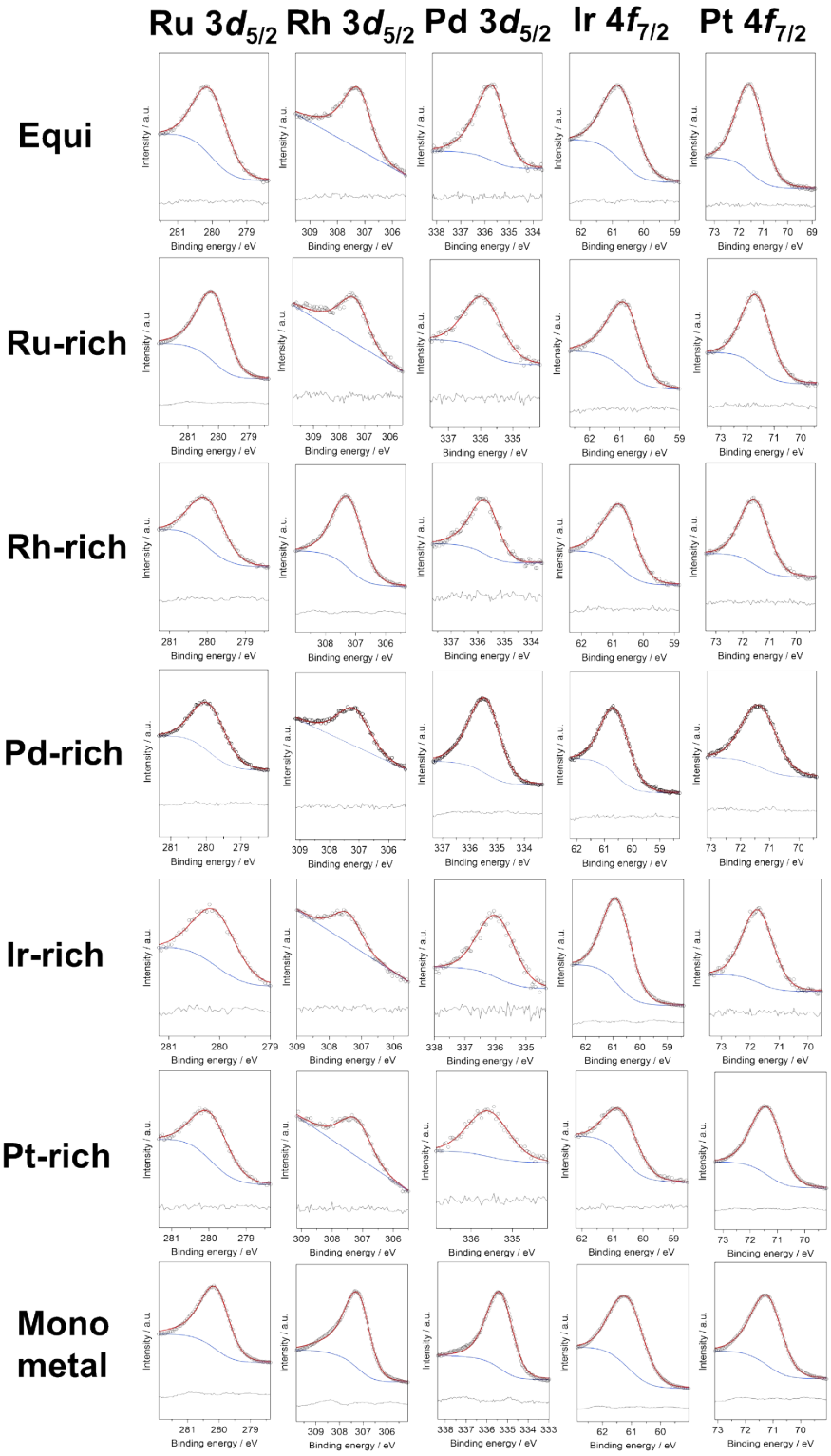

Fig. S6. XPS spectra (black circles) and fitting curves (red lines). The linear (Rh) and Shirley (the others) background curves are shown by blue curves. Peak positions are summarised in Table S2.

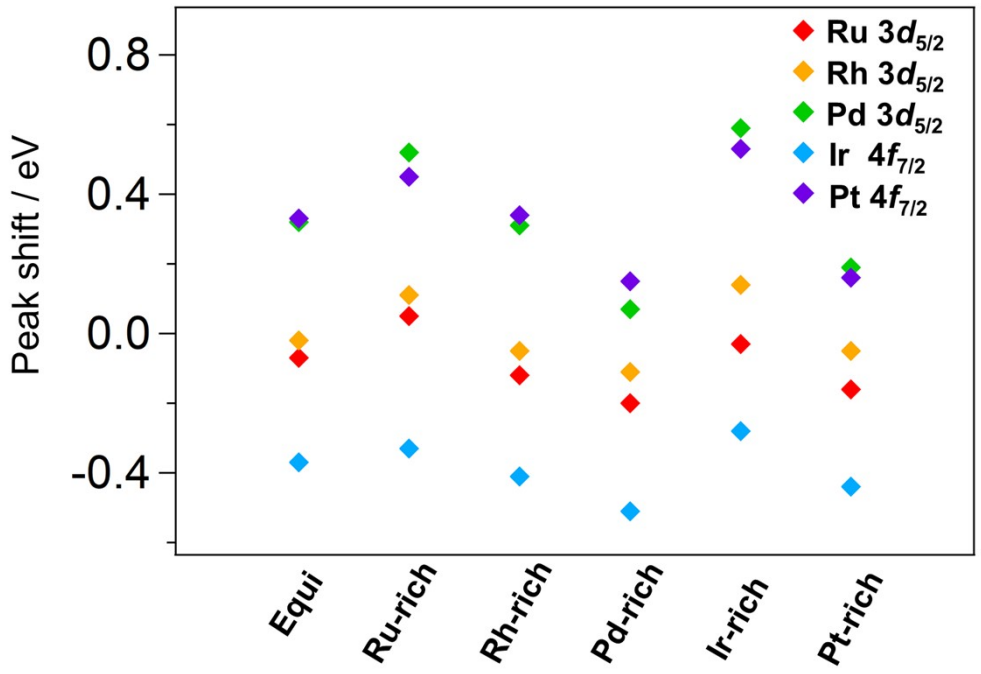

Fig. S7. Peak shift of XPS core level spectra of the alloy NPs from monometallic NPs.

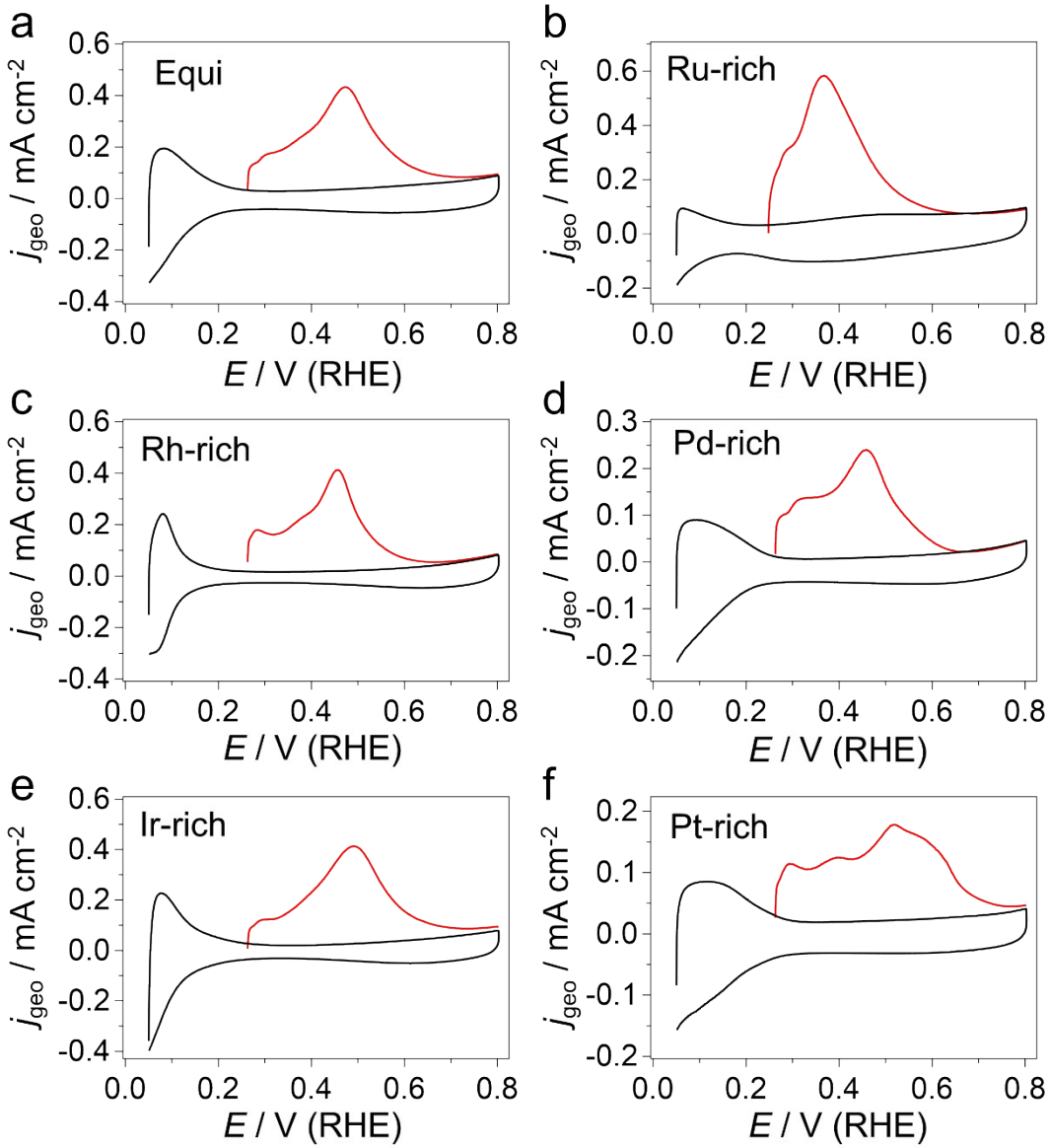

Fig. S8. Cu UPD measurements for (a) Equi, (b) Ru-rich, (c) Rh-rich, (d) Pd-rich, (e) Ir-rich and (f) Pt-rich alloy NPs. Red curves show Cu UPD, and black curves show the background measured in pure 0.5 M H_2SO_4 (aq). EASA is summarised in Table S4.

Table S1. The precursors amount for each sample.

	$RuCl_3 \cdot nH_2O$	$RhCl_3 \cdot nH_2O$	K_2PdCl_4	H_2IrCl_6	K_2PtCl_4
Equi	12.9	15.1	18.7	24.2	23.3
Ru-rich	52.2	8.8	10.9	14.0	13.8
Rh-rich	8.6	52.1	10.8	13.9	13.7
Pd-rich	8.5	8.6	63.7	13.6	13.5
Ir-rich	6.3	6.4	7.9	52.9	10.0
Pt-rich	6.3	6.3	7.8	10.0	59.6
Ru	89.3	0	0	0	0
Rh	0	102.4	0	0	0
Ir	0	0	0	87.4	0
Pt	0	0	0	0	85.1

(mg)

Table S2. Comparison of crystallite sizes obtained from PXRD, and particle sizes obtained from TEM.

	Crystallite size (nm)	Particle size (nm)
Equimolar	3.98 ± 0.02	4.6 ±1.7
Ru-rich	2.62 ± 0.01	3.6 ± 1.6
Rh-rich	6.62 ± 0.03	4.0 ± 1.6
Pd-rich	6.20 ± 0.03	4.6 ± 2.0
Ir-rich	2.70 ± 0.10	3.0 ± 0.7
Pt-rich	5.99 ± 0.02	4.4 ± 1.7

Table S3. Peak positions of core-level XPS spectra

	Ru $3d_{5/2}$	Rh $3d_{5/2}$	Pd $3d_{5/2}$	Ir $4f_{7/2}$	Pt $4f_{7/2}$
Equi	280.04	307.26	335.71	60.75	71.53
Ru-rich	280.16	307.39	335.91	60.79	71.65
Rh-rich	279.99	307.23	335.7	60.71	71.54
Pd-rich	279.99	307.23	335.53	60.67	71.38
Ir-rich	280.08	307.42	335.98	60.84	71.73
Pt-rich	279.95	307.23	335.58	60.68	71.36
Monometal	280.11	307.28	335.36	61.12	71.20

(eV)

Table S4. *d*-band centre of the obtained NPs

Equi	Ru-rich	Rh-rich	Pd-rich	Ir-rich	Pt-rich
-4.089	-4.111	-4.066	-3.922	-4.142	-4.106
Ru	Rh	Pd	Ir	Pt	
-4.042	-3.866	-3.443	-4.294	-4.038	

Table S5. EASA of the obtained alloy NPs

Equi	Ru-rich	Rh-rich	Pd-rich	Ir-rich	(eV)
74.9	83.0	62.6	42.1	76.6	43.6

(m^2/g)